



Intramolecular N...F Pnictogen Bond Mitigates the Explosive Behavior of Azido-L-Phenylalanines

Andrea Pizzi, Eleonora Veronese, Nicola Demitri, Marco Saccone,* Pierangelo Metrangolo,* and Giancarlo Terraneo*

Dedicated to Professor Giuseppe Resnati on the occasion of his 70th birthday

Organic azides are versatile intermediates but are plagued by intrinsic instability and potential explosiveness. Here, it is shown that fluorinated azido-L-phenylalanines display unexpected stability, arising from adjacent fluorine atoms that enforce intramolecular pnictogen bonding. Single-crystal X-ray diffraction reveals an intramolecular N...F pnictogen bond that orients the azide

group and enhances molecular stability. Comparison with non-fluorinated analogs underscores the stabilizing effect of fluorine substitution in mitigating explosive decomposition. Quantum chemical and bond critical point analyses corroborate the stabilizing role of the N...F pnictogen bond.

1. Introduction

Organic azides are a class of energy-rich compounds that, thanks to their simple and robust chemistry, have been widely used in different research fields as diverse as blowing agents or functional intermediates in pharmaceuticals.^[1–3] Although organic azides are intrinsically energy-rich and may display explosive behavior, their exceptional reactivity has made them invaluable synthetic intermediates. Since the discovery of the copper(I)-catalyzed azide–alkyne cycloaddition (CuAAC),^[4–6] the so-called "click reaction," the use of organic azides has expanded dramatically—particularly in peptide and biomaterial chemistry—owing to its remarkable efficiency, selectivity, and compatibility with aqueous and biological environments. In parallel, the topochemical azide–alkyne cycloaddition (TAAC)^[7–9] has further

extended the versatility of azide–alkyne click chemistry, enabling the construction of polymers and supramolecular architectures from azide-functionalized peptides, carbohydrates, and nucleic acids with outstanding structural precision and functional diversity. Together, CuAAC- and TAAC-based strategies underscore the central role of azide chemistry in the modular design of advanced peptide-based materials.^[10–13]

In this framework, one of the main trends in peptide-based nanotechnology consists in combining new and efficient functionalities with extreme structural simplicity: the reductionist approach.^[14] Along with the 20 natural amino acids, non-natural amino acids—including the ones containing azido groups—are largely employed to further enlarge the chemical and structural diversity in the peptide field. The azide-containing amino acids are not only key precursors for cycloaddition reactions, but also become important intermediates for the introduction of other chemical groups. For example, in 2012, an elegant synthetic strategy enabled the preparation of a series of *para*-X-tetrafluorophenylalanines, where X was a wide range of chemical groups, including the azide moiety, which was used as an intermediate for the formation of amino group.^[15]

Recently, it has emerged that the chemical modification of the aromatic unit in a halogenated phenylalanine fragment could play a crucial role in defining its supramolecular behavior and chemical properties.^[16,17] For instance, upon changing the number, position, and nature of the halogen atoms introduced in the phenyl moiety, it was possible to tune the self-assembly phenomena of the short peptide sequences.^[18–21] Further, the substitution of the hydrogen atoms with fluorine atoms on the aromatic unit of the 4-iodo-L-phenylalanine led to the activation of the iodine atom, making the halogenated amino acid an efficient catalyst for the aqueous synthesis of bis-(heterocyclic)methane.^[22]

Notably, during the synthesis 4-iodo-2,3,5,6-tetrafluoro-L-phenylalanine catalyst, we observed an unexpected good

A. Pizzi, E. Veronese, P. Metrangolo, G. Terraneo
Department of Chemistry
Materials and Chemical Engineering "Giulio Natta" Politecnico di Milano
Laboratory of Supramolecular and Bio-Nanomaterials (SBNLab)
Via Luigi Mancinelli 7, 20131 Milano, Italy
E-mail: pierangelo.metrangolo@polimi.it
giancarlo.terraneo@polimi.it

N. Demitri
Elettra-Sincrotrone Trieste S.C.P.A
Basovizza, 34149 Trieste, Italy

M. Saccone
Dipartimento di Scienze e Innovazione Tecnologica
Università del Piemonte Orientale
Viale Teresa Michel 11, 15121 Alessandria, Italy
E-mail: marco.saccone@uniupo.it

Supporting information for this article is available on the WWW under <https://doi.org/10.1002/ceur.202500371>

© 2025 The Author(s). ChemistryEurope published by Chemistry Europe and Wiley-VCH GmbH. This is an open access article under the terms of the Creative Commons Attribution License, which permits use, distribution and reproduction in any medium, provided the original work is properly cited.



chemical stability of its intermediate, the *N*-Boc-4-azido-2,3,5,6-tetrafluoro-L-phenylalanine tert-butyl ester (**1**, Scheme 1). This contrasts literature reports suggesting that electron-withdrawing fluorine substituents adjacent to azides should enhance reactivity and decrease stability,^[23–25] a fact that promoted their use as phenylazide-labeling (PAL) reagents.^[24] To clarify the stabilizing influence of *ortho*-fluorine atoms on azido groups, we investigated the structure–property relationships of the potentially explosive *N*-Boc protected (**1**) and the unprotected 4-azido-2,3,5,6-tetrafluoro-L-phenylalanine (**2**, Scheme 1).

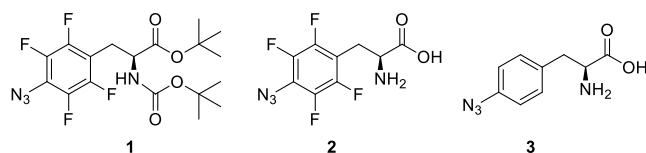
Herein, we study, through differential scanning calorimetry (DSC) and X-ray diffraction analysis, the solid-state behavior of the two fluorinated L-phenylalanine **1** and **2** and show how the presence of an intramolecular N...F contact, namely a pnictogen bond (PnB),^[26] could be responsible for the enhanced thermal stability of the obtained fluorinated peptides. In addition, the nonfluorinated 4-azido-phenylalanine (**3**) was analyzed to evaluate the structural differences with its fluorinated analogs.

2. Results and Discussion

Azide **1** was synthesized following the procedure reported in ref. [22] and after its purification by crystallization from dichloromethane, it was deprotected to get the 4-azido-2,3,5,6-tetrafluoro-L-phenylalanine **2** (I section S1, Supporting Information). The thermal stability, and therefore the potential explosive behavior, of compounds **1** and **2** was first assessed by DSC analysis. It is known that DSC could give a reliable indication of the decomposition energy, when released upon heating, by an energy-rich compound.^[27] In fact, the presence of a very pronounced exothermic peak in the DSC thermogram indicates a fast decomposition process which is, for azides, generally associated to a possible explosive behavior. In addition, the DSC data can be used to have an estimation of two important parameters for the classification of the explosive compounds, which are the shock sensitivity (*SS*, (Equation 1)) and the explosive propagation (*EP*, Equation(2)), respectively. Specifically, the total measured energy (*Q*, cal/g) and the onset temperatures (*T*, °C) of the exothermic peaks, extrapolated from DSC thermogram, allow the calculation of *SS* and *EP* through Yoshida's correlations:^[28]

$$SS = \log 10Q - 0.72 \cdot \log(T - 25) - 0.98 \quad (1)$$

$$EP = \log 10Q - 0.38 \cdot \log(T - 25) - 1.67 \quad (2)$$



Scheme 1. Chemical structures of the studied compounds: *N*-Boc-(4-azido-2,3,5,6-tetrafluoro)-L-phenylalanine tert-butyl ester (**1**), 4-azido-2,3,5,6-tetrafluoro-L-phenylalanine (**2**), and 4-azido-L-phenylalanine (**3**).

Table 1. DSC analysis (onset *T* of the exothermic peak), *SS*, and *EP* values calculated from DSC using Yoshida's correlations.

Compound	Released energy ^{a)}	<i>T</i> ^{b)}	<i>SS</i>	<i>EP</i>
1	63	165	−0.73	−0.69
2	58	152	−0.73	−0.71
3	274 ^{c)}	139 ^{c)}	−0.01 ^{c)}	−0.02 ^{c)}

^{a)}cal/g. ^{b)}°C. ^{c)}From ref. [29].

The analysis of the DSC thermograms, by equations 1 and 2, of the amino acids **1** and **2** showed negative values for both *SS* and *EP* parameters (Table 1 and Figure S4,5, Supporting Information), which were in counter-tendency to the common behavior of explosive compounds where the two indices are equal or greater than zero.^[27,28]

Specifically, data in Table 1 suggested that the replacement of the hydrogen atoms of the aromatic ring with fluorine atoms sensibly decreased the shock sensitivity and explosive propagation behavior of the fluorinated amino acids compared to the hydrogenated system **3**.^[29] In addition, the released energy value of the hydrogenated 4-azido-L-phenylalanine **3** was five times higher than **1** and **2**, further proving how the presence of the fluorinated moiety close to the azide group played a key role in the chemical stabilization of the compounds, mitigating the risk of explosion and thus facilitating the handling and storage of these materials. We wish to point out that the sensitivity properties of potentially dangerous organic azides, such as **3**, in terms of decomposition temperatures, have also been studied computationally, and good agreement has been observed with the experimental data.^[30]

After these initial findings, we focused on the analysis of the crystal structures of **1** and **2**, aiming to get a structural insight on the possible role of the fluorine atoms in the stabilization of the azide units (Table S1, Supporting Information). Needle-shaped crystals of **1** suitable for single-crystal X-ray diffraction were obtained after a few days of slow evaporation from a dichloromethane (DCM) solution. Compound **1** crystallized in the orthorhombic *P*2₁2₁2₁ space group, with a single amino acid molecule in the asymmetric unit. The peptides were assembled thanks to classical hydrogen bond (HB) interaction (the distance N3...O4 is 3.108(2)Å involving the amide units of adjacent molecules, which led to the formation of an infinite hydrogen-bonded chain running along the crystallographic *a*-axis. In addition, the oxygen atom O4 established in a hydrogen-bonding interaction with the hydrogen atoms of the benzylic carbon and a π -hole interaction^[31] with the carbon atom of the C=O group (Figure 1). These contacts promoted the isotactic arrangement of the 4-azido-2,3,5,6-tetrafluorobenzene units in the supramolecular chain, placing them opposite to the bulky Boc groups.

Interestingly, the fluorine atoms on the aromatic ring were involved in several intermolecular and intramolecular contacts, which stabilized the overall crystal packing (Figure 1). The fluorine atom (F1) of one molecule interacted either with one methyl hydrogen of the *t*Bu unit (F1...H14C, distance 2.578 Å) and with a carbon atom of the aromatic ring of an adjacent amino acid (F1...C7, distance 3.130(3) Å). The latter interaction is the classical

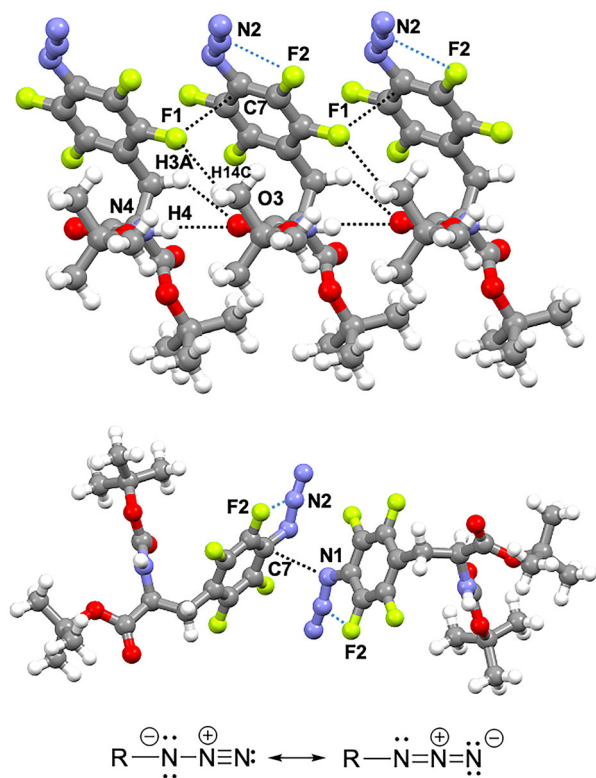


Figure 1. (Top) Crystallographic representation of the hydrogen-bonded chain of compound 1 where the intrachain Pn contacts involving fluorine atoms are also highlighted. (Middle) Dimer of compound 1 where the PnB and intermolecular interaction involving the azide group are shown. (Bottom) Resonance structures of the substituted azide that show the charge distribution on the $-\text{N}_3$ group. Noncovalent interactions are shown in light blue and black dotted lines for PnBs and HBs, respectively. Dihedral angle $\varphi_{\text{C}-\text{C}-\text{N}-\text{N}} = -13.9^\circ$ in 1. Color code: C, gray; O, red; N, violet; F, yellow; and H, white.

offset parallel arrangement of two fluorinated aromatic rings, where the electron density of the fluorine atom points toward the depleted electron density area on the surface of an adjacent fluorinated benzene.^[32]

Notably, the fluorine atom (F2) in *ortho* position to the azide group formed a short intramolecular contact with nitrogen atom (N2) of the $-\text{N}_3$ unit (N2...F2 distance 2.638(3) Å, which corresponds to a normalized contacts (Nc)^[33] of 0.85 (Figure 1 middle). We will show below through quantum chemical methods how significant this kind of interaction is from the energetic point of view. The azido group can be written using two resonance forms, where the central nitrogen atom has positive charge (Figure 1, bottom). In these forms, the positively charged central N functioned as electron density acceptor site, namely pnictogen bonding donor, interacting with the electron density provided by the close fluorine atom.^[34] The intramolecular N...F pnictogen bond dictated the orientation of the $-\text{N}_3$ unit, creating a five-member supramolecular ring. This five-membered intramolecular arrangement resembles the orientation patterns observed between azide units and chalcogen or pnictogen atoms recently reported in related systems,^[35] further supporting the structural analogy and reinforcing the notion that such directional noncovalent forces govern azide orientation. Thus, the presence of the

intramolecular N...F PnB interaction could be responsible for the increased stability of the azide unit, mitigating the risk of explosion. It is also worth to notice that the nitrogen atom (N1) was in contact with the carbon atom (C7) of a close amino acid which belonged to an adjacent peptide unit (N1...C7, distance 3.216(3) Å and Nc = 0.94, Figure 1 middle). As in the previous interaction, the inverted quadrupole moment of the fluorinated benzene promoted the electrophilic nature of the carbon atom, thus enhancing its ability to interact with an electron density provided by the N1 atom.

The following step was the removal of the Boc protecting group to evaluate the influence of this unit on the overall stability of the azido amino acid. Unfortunately, the solubility of the

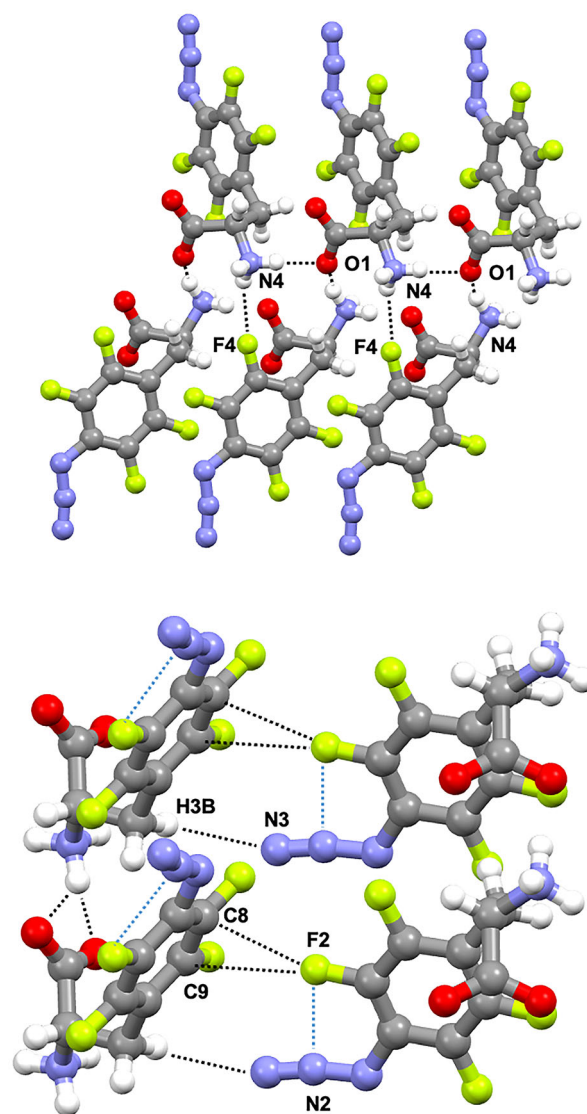


Figure 2. Crystallographic representation of: (Top) the hydrogen-bonded network of compound 2 where the intrachain contacts involving fluorine atoms and $-\text{NH}_3^+$ units are also highlighted; (Bottom) the packing arrangement of adjacent H-bonded chains promoted by a T-shape interaction between two fluorinated rings and the intramolecular PnB and intermolecular interaction involving the azide group are shown. Dihedral angle $\varphi_{\text{C}-\text{C}-\text{N}-\text{N}} = -2.2^\circ$ in 2. Noncovalent interactions and color code as in Figure 1.



unprotected peptide **2** drastically dropped in chlorinated solvents, and the single crystals were exclusively obtained from a dimethyl sulfoxide (DMSO) solution.

As for **1**, the compound **2** crystallized in the orthorhombic $P2_12_12_1$ space group but as a DMSO solvate with a single amino acid molecule in the asymmetric unit. The unprotected peptide crystallized in its zwitterionic form and assembled thanks to the charged-assisted hydrogen bonding interaction occurring between the -NH_3^+ unit and the carboxylate group. Specifically, the oxygen atom (O1) acted as a bidentate electron density donor site interacting with two ammonium units of two different amino acids ($\text{O1}\cdots\text{N4}_{(-1+x, y, z)}$, distance 2.702(2) Å and $\text{O1}\cdots\text{N4}_{(-0.5+x, 1.5-y, 1-z)}$, distance 2.945(3) Å). This feature elicited the formation of a hydrogen-bonded ribbon, which propagated along the crystallographic a -axis (Figure 2 top).

Thanks to the pairing of the charged groups, the 4-azido-2,3,5,6-tetrafluorobenzene moieties stood up from the supramolecular backbone as alternating prongs. In the hydrogen-bonded backbone, the presence of short F \cdots H contacts involving the fluorine atom (F4) and the -NH_3^+ unit further stabilized the supramolecular ribbon, tightening together the amino acid units ($\text{F4}\cdots\text{N4}$, distance 2.891(2) Å, Figure 2 top). The DMSO molecule was also hydrogen-bonded to the -NH_3^+ unit. The packing of the H-bonded ribbons was promoted by a T-shape interaction occurring

between two fluorinated rings (F2 \cdots Centroid C8-C9 bond, distance 3 Å, Figure 2 bottom).

Even in **2**, the azido unit was involved in two noncovalent contacts, one intramolecular and one intermolecular. The intramolecular pnictogen bond took place between the fluorine atom (F2) and the nitrogen atom (N2), mirroring the geometrical features of the PnB detected in **1** (N2 \cdots F2 distance 2.636(3) Å, $\text{Nc} = 0.85$). The PnB imposed the orientation of the -N_3 unit, which adopted a coplanar arrangement with the tetrafluorophenyl ring as seen in **1**.

To assess whether the formation of the intramolecular PnB in the 4-azido-2,3,5,6-tetrafluorophenyl moiety was a general supramolecular feature, we performed a structural search into the Cambridge Structural Database (CSD)^[36] looking for the N \cdots F contacts, where the nitrogen atom belongs to the -N_3 unit.

Interestingly, all the reported structures (19 entries) showed an intramolecular pnictogen bond occurring between the nitrogen atom in the central position of the azo group and the fluorine atom placed in its *ortho* position with geometrical parameters identical to those found in **1** and **2** (N \cdots F, 2.642 Å average distance, Figure 3 and Supporting Information). Even in all CSD structures, the -N_3 group adopted a coplanar arrangement with the tetrafluorophenyl ring creating, through the PnB, a five-member supramolecular ring. These findings suggested a strong

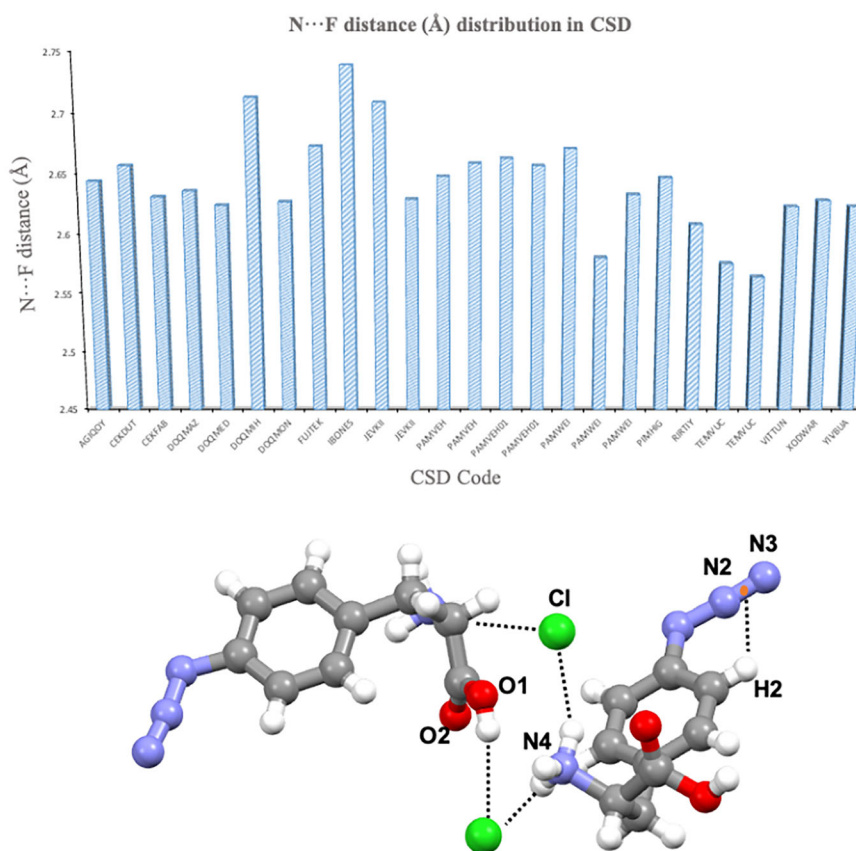


Figure 3. (Top) Histogram chart of intramolecular N \cdots F PnB in CSD. (Bottom) Crystallographic representation of hydrogen-bonded dimer for compound **3**. I Dihedral angle $\varphi_{\text{C-C-N-N}} = 4^\circ$ in **3**. Inter- and intramolecular interactions are highlighted and color code as in Figure 1, Cl, green. N2=N3 centroid is shown as an orange dot.

tendency to form an intramolecular N \cdots F PnB whenever a fluorine atom is in *ortho* position to an -N $_3$ on an aromatic ring, regardless of the chemical nature of the remaining part of the molecule. The analysis of the nonfluorinated 4-azido-phenylalanine (**3**) was conducted to assess the structural differences compared to its fluorinated analogs. Compound **3** crystallized in the monoclinic $P2_1$ space group as chloride derivative. The overall assembly was driven by multiple hydrogen bonds occurring between the ammonium unit and the chloride anion and the carboxylic group (Figure 3 and Supporting Information). The most interesting aspect was the position and the noncovalent interactions involving the -N $_3$ group. Even in the nonfluorinated sample, the azo group was placed on the same plane described by the aromatic ring, which assumes the same conformation seen in **1** and **2**. However, in this case, the arrangement of the -N $_3$ unit was stabilized by the presence of an intramolecular $\pi\cdots$ H2 contact occurring between the π cloud of the -N $_3$ group and the hydrogen atom in its *ortho* position (Centroid N2=N3 \cdots H2 distance 2.538 Å, Figure 3).

To better understand the effect of the fluorination on the 4-azido-phenyl moiety, we performed quantum chemical calculations on **2** and **3** (see SI for full technical details). We initially performed a conformational stability test on the position of the azide group in **2** and **3**, tilting by 90° the -N $_3$ unit out of the plane containing the aromatic unit (dihedral angle $\phi_{C-C-N-N} = 0$ and 90°) and then comparing the energy of the untilted and tilted conformation. (Figure 4 and S12). The calculations showed that the fluorinated structure **2** was destabilized by 25.91 kJ mol $^{-1}$ by tilting the azido unit away from the coplanar position, while the hydrogenated structure was destabilized by 23.34 kJ mol $^{-1}$. This finding showed that the most stable conformation for the -N $_3$ unit was the native one (namely, when the -N $_3$ unit adopted a coplanar arrangement with the phenyl ring) for both structures, and highlighted that the perfluorinated azide structure in its native conformation was more stable compared to the hydrogenated azide. The stability was provided by the presence of the intramolecular PnB in the fluorinated system **2**.

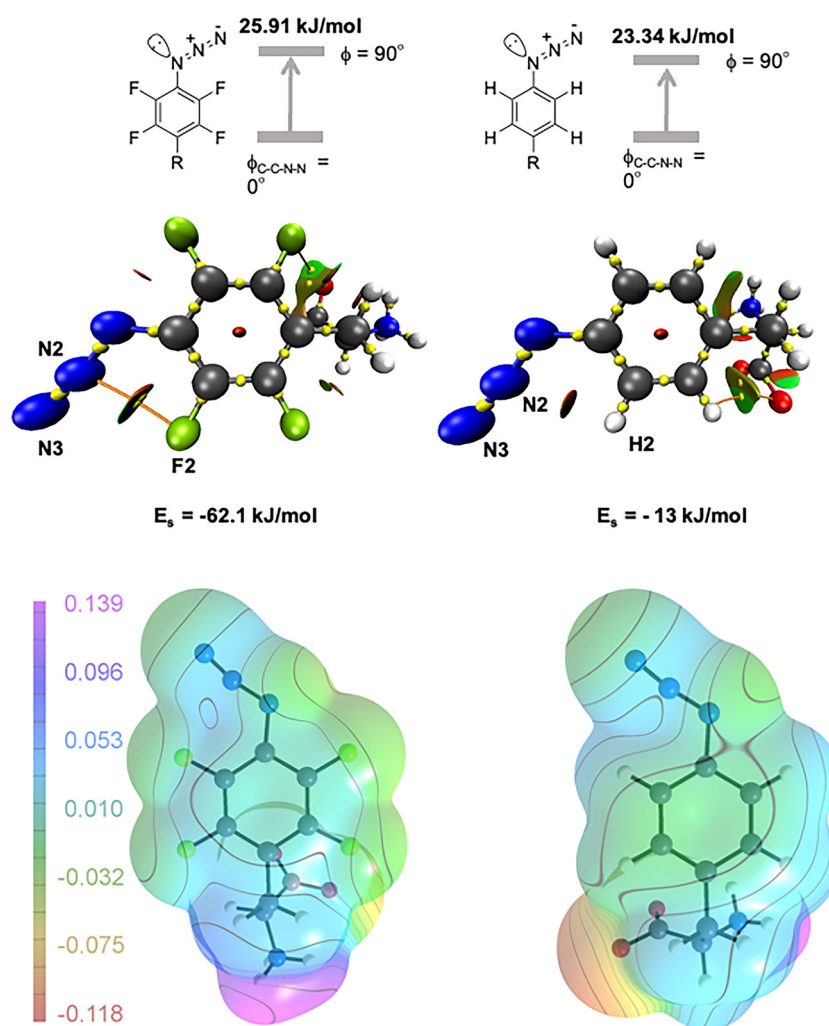


Figure 4. Top: schematic view of the destabilization of **2** and **3** caused by the tilting of their azide groups. Middle: NCI-QTAIM of **2** and **3** with the associated BCPs and interaction energies calculated with the IQA. Bottom: molecular electrostatic potential maps of **2** and **3** plotted on the 0.001 au contour of the electron density (values in Hartrees).



Non-covalent interactions^[37] analysis associated with the quantum theory of atoms-in-molecules (QTAIM) analysis^[38] of bond critical points (BCPs) was then employed to provide qualitative hints on the intramolecular interaction pattern in **2** and **3**. Notably, in **2**, a BCP was observed between the F atom of the central N atom in the azide group, while a BCP was absent in structure **3** when the F atom is substituted with a H atom (Figure 4 and see S11, Supporting Information). Although the presence of a BCP does not always guarantee an attractive interaction between two atoms or moieties,^[39] quantitative results on the energies involved were provided by interacting quantum atoms (IQA)^[40] calculations, which have been proven to be a reliable method to quantify the intramolecular interactions involving perfluorinated aromatic units.^[41] In particular, we focused on the interactions between F2...N2 and F2...N3 in structure **2** and H2...N2 and H2...N3 in structure **3** (Figure 4). We wish to point out that the IQA analysis provides the interaction energy between two atoms, which is not directly comparable with the supramolecular method, in which the interaction energy between two molecules is computed by calculating the energy of the molecules together and subtracting the energies of the separated monomers.

The sum of interaction energies for both the N...F contacts in **2** yielded a stabilization energy (E_s) of $-62.1 \text{ kJ mol}^{-1}$ with an almost equal contribution from coulombic and exchange-correlation parts (see Supporting Information), while the stabilization energy for the N...H interactions in **3** was only $-13.0 \text{ kJ mol}^{-1}$ which came exclusively from exchange-correlation contributions, while the coulombic part is repulsive (see Supporting Information). The qualitative impact of the coulombic contribution was also visible in molecular electrostatic potential maps of both **2** and **3** (see Figure 4). These digits provided clear evidence of the fundamental role of the N...F PnB in stabilization of the azido unit, mitigating its explosive behavior.

3. Conclusion

In conclusion, this study focused on investigating the structural stability of fluorinated peptides containing azide groups. The presence of fluorine atoms in *ortho* position to the azido groups enhanced the stability of the compounds. Through thermal and X-ray diffraction analysis, it was revealed that intramolecular N...F pnictogen bonds played a crucial role in enhancing the stability of fluorinated peptides. Comparison with nonfluorinated analogs highlights fluorine's decisive role in mitigating explosive behavior. Crystallographic analysis revealed the presence of intramolecular PnBs, which dictated the orientation of the azide unit and contributed to the overall stability of the compounds, while QTAIM calculations further supported the role of PnBs in stabilizing fluorinated peptides.

The findings underscore the importance of understanding the structure–stability relationships between azide units and their noncovalent interactions with different molecular entities,^[42–46] in line with previous studies by Akeröy et al. on solid-state energetic materials.^[47,48] The present work further expands the fundamental knowledge of how specific noncovalent interactions

influence the stability of energetic systems, thereby contributing to the rational design and safer manipulation of peptide-based energetic materials.

Supporting Information

The authors have cited additional references within the Supporting Information.^[49–64]

Acknowledgements

XRD data for **1** and **2** were collected under Elettra Sincrotrone beamtime proposal No. 2018548.

Conflict of Interest

The authors declare no conflict of interest

Data Availability Statement

The data that support the findings of this study are available from the corresponding author upon reasonable request.

Keywords: azide stability · fluorinated peptides · pnictogen bond (PnB)

- [1] S. Bräse, C. Gil, K. Knepper, V. Zimmermann, *Angew. Chemie Int. Ed.* **2005**, *44*, 5188.
- [2] K. Bozorov, J. Zhao, H. A. Aisa, *Bioorganic Med. Chem.* **2019**, *27*, 3511.
- [3] D. Huang, G. Yan, *Adv. Synth. Catal.* **2017**, *359*, 1600.
- [4] C. Wang, D. Ikhlef, S. Kahlal, J. Saillard, *Coord. Chem. Rev.* **2016**, *316*, 1.
- [5] E. Haldón, M. C. Nicasio, P. J. Pérez, *Org. Biomol. Chem.* **2015**, *13*, 9528.
- [6] J. E. Hein, V. V. Fokin, *Chem. Soc. Rev.* **2010**, *39*, 1302.
- [7] H. Kuntrapakam, K. M. Sureshan, *Acc. Chem. Res.* **2019**, *52*, 3149.
- [8] B. P. Krishnan, K. M. Sureshan, *J. Am. Chem. Soc.* **2017**, *139*, 1584.
- [9] V. Athiyarath, L. A. Mathew, Y. Zhao, R. Khazeber, U. Ramamurty, K. M. Sureshan, *Chem. Sci.* **2023**, *14*, 5132.
- [10] O. Boutureira, G. J. L. Bernardes, *Chem. Rev.* **2015**, *115*, 2174.
- [11] A. A. H. A. Fuaad, F. Azmi, M. Skwarczynski, I. Toth, *Molecules* **2013**, *18*, 13148.
- [12] W. Li, Z. Wang, F. Deschler, S. Gao, R. H. Friend, A. K. Cheetham, *Nat. Rev. Mater.* **2017**, *2*, 16099.
- [13] A. Nagai, Z. Guo, X. Feng, S. Jin, X. Chen, X. Ding, D. Jiang, *Nat. Commun.* **2011**, *2*, <https://doi.org/10.1038/ncomms1542>.
- [14] E. Gazit, *Annu. Rev. Biochem.* **2018**, *87*, 533.
- [15] L. Qin, C. Sheridan, J. Gao, *Org. Lett.* **2012**, *14*, 528.
- [16] A. Pizzi, L. Lascialfari, N. Demitri, A. Bertolani, D. Maiolo, E. Carretti, P. Metrangolo, *CrystEngComm* **2017**, *19*, 1870.
- [17] A. Bertolani, L. Pirrie, L. Stefan, N. Houbenov, J. S. Haataja, L. Catalano, G. Terraneo, G. Giancane, L. Valli, R. Milani, O. Ikkala, G. Resnati, P. Metrangolo, *Nat. Commun.* **2015**, *6*, 1.
- [18] A. Pizzi, C. Pigliacelli, A. Gori, N. Nonappa, O. Ikkala, N. Demitri, G. Terraneo, V. Castelletto, I. W. Hamley, F. B. Bombelli, P. Metrangolo, *Nanoscale* **2017**, *9*, 9805.
- [19] A. Bertolani, A. Pizzi, L. Pirrie, L. Gazzera, G. Morra, M. Meli, G. Colombo, A. Genoni, G. Cavallo, G. Terraneo, G. Terraneo, P. Metrangolo, *Chem. - Eur. J.* **2017**, *23*, 2051.
- [20] A. Pizzi, N. Demitri, G. Terraneo, P. Metrangolo, *CrystEngComm* **2018**, *20*, 5321.
- [21] A. Pizzi, V. Dichiarante, G. Terraneo, P. Metrangolo, *Pept. Sci.* **2018**, *110*, <https://doi.org/10.1002/bip.23088>.



- [22] G. Bergamaschi, L. Lascialfari, A. Pizzi, M. I. M. Espinoza, N. Demitri, A. Milani, A. Gori, P. Metrangolo, *Chem. Commun.* **2018**, *54*, 10718.
- [23] K. G. Pinney, J. A. Katzenellenbogen, *J. Org. Chem.* **1991**, *56*, 3125.
- [24] N. Soundararajan, M. S. Platz, *J. Org. Chem.* **1990**, 2034.
- [25] J. Zhang, Y. Gao, X. Kang, Z. Zhu, Z. Wang, Z. Xi, L. Yi, *Org. Biomol. Chem.* **2017**, *15*, 4212.
- [26] G. Resnati, D. L. Bryce, G. R. Desiraju, A. Frontera, I. Krossing, A. C. Legon, P. Metrangolo, F. Nicotra, K. Rissanen, S. Scheiner, G. Terraneo, *Pure Appl. Chem.* **2024**, *96*, 135.
- [27] P. Folly, *Chimia Aarau* **2004**, *58*, 394.
- [28] M. Yoshida, T. Yoshizawa, F. Itoh, M. Matsunaga, T. Watanabe, M. Tamura, *Kogyo Kagaku* **1987**, *48*, 311.
- [29] M. B. Richardson, D. B. Brown, C. A. Vasquez, J. W. Ziller, K. M. Johnston, G. A. Weiss, *J. Org. Chem.* **2018**, *83*, 4525.
- [30] J. Rein, J. M. Meinhardt, J. L. H. Wahlman, M. S. Sigman, S. Lin, *Angew. Chem. Int. Ed.* **2023**, *62*, e202218213.
- [31] P. Politzer, J. S. Murray, T. Clark, *Phys. Chem. Chem. Phys.* **2021**, *23*, 16458.
- [32] C. J. Pace, J. Gao, *Acc. Chem. Res.* **2013**, *46*, 907.
- [33] The normalized contact (Nc) for an interaction between atoms i and j is the ratio $D_{ij}/(r_{vdW,i} + r_{vdW,j})$ where D_{ij} is the experimental distance between i and j and $r_{vdW,i}$ and $r_{vdW,j}$ are the van der Waals radii of i and j. Nc values smaller than 1 indicates attractive interactions, vdW Radii used here: H=1.20, C=1.77, N=1.66, O=1.50, F=1.46 Å.
- [34] S. Scheiner, *J. Phys. Chem. A.* **2021**, *125*, 10419.
- [35] M. Bursch, L. Kunze, A. M. Vibhute, A. Hansen, K. M. Sureshan, P. G. Jones, S. Grimme, D. B. Werz, *Chem. Eur. J.* **2021**, *27*, 4627.
- [36] C. R. Groom, I. J. Bruno, M. P. Lightfoot, S. C. Ward, *Acta Crystallogr. Sect. B Struct. Sci. Cryst. Eng. Mater.* **2016**, *72*, 171.
- [37] E. R. Johnson, S. Keinan, P. Mori-Sánchez, J. Contreras-García, A. J. Cohen, W. Yang, *J. Am. Chem. Soc.* **2010**, *132*, 6498.
- [38] R. F. W. Bader, *Chem. Rev.* **1991**, *91*, 893.
- [39] A. Gavezzotti, *Advanced X-ray Crystallography*, K. Rissanen, Springer Berlin Heidelberg, Berlin, Heidelberg **2012**, 1–32.
- [40] M. A. Blanco, A. M. Pendás, E. Francisco, *J. Chem. Theory Comput.* **2005**, *1*, 1096.
- [41] M. Saccone, A. Siiskonen, F. Fernandez-Palacio, A. Priimagi, G. Terraneo, G. Resnati, P. Metrangolo, *Acta Crystallogr. Sect. B Struct. Sci. Cryst. Eng. Mater.* **2017**, *73*, 227.
- [42] M. C. Madhusudhanan, H. Balan, D. B. Werz, K. M. Sureshan, *Angew. Chemie—Int. Ed.* **2021**, *60*, 22797.
- [43] B. Lin, H. Liu, I. Karki, E. C. Vik, M. D. Smith, P. J. Pellechia, K. D. Shimizu, *Angew. Chemie—Int. Ed.* **2023**, *62*, 1.
- [44] T. Yamashiro, T. Abe, M. Tanioka, S. Kamino, D. Sawada, *Chem. Commun.* **2021**, *57*, 13381.
- [45] S. Bhandary, A. Pathigoolla, M. C. Madhusudhanan, K. M. Sureshan, *Chem. - A Eur. J.* **2022**, *28*, <https://doi.org/10.1002/chem.202200820>.
- [46] C. Raju, S. Kunnikuruvan, K. M. Sureshan, *Angew. Chemie—Int. Ed.* **2022**, *61*, 1.
- [47] M. D. Perera, A. S. Sinha, C. B. Aakeröy, *Can. J. Chem.* **2020**, *98*, 358.
- [48] J. C. Gamekkanda, A. S. Sinha, C. B. Aakeröy, *Crystal Growth & Design* **2020**, *20*, 2432.

Manuscript received: September 11, 2025

Revised manuscript received: November 4, 2025

Version of record online: